

A Comparative Study of Bilinear Time–Frequency Transforms of ISAR Signals for Air Target Imaging

G. E. Bouladakis, G. K. Kalognomos, A. V. Karakasiliotis, P. V. Frangos

Division of Information Transmission Systems and Materials Technology, School of Electrical and Computer Engineering, National Technical University of Athens

9 Iroon Polytechniou Street, Zografou, GR 15773, Athens, Greece, phone: +30 2107723694,

e-mails: geoboult@ontelecoms.gr, pfrangos@central.ntua.gr, kalognomos@ieee.org, anastasiskarak@yahoo.gr

L. K. Stergioulas

Brunel University, Uxbridge, Middlesex

UB8 3PH, United Kingdom, e-mail: Lampros.Stergioulas@brunel.ac.uk

Introduction

Among the literally countless ways of representing a signal, two-dimensional representations in both time and frequency by means of so-called joint ‘time-frequency’ (TF) signal distributions have recently enjoyed a growing popularity, for rapidly varying non-stationary signals [1,2].

Time-Frequency Transforms were developed for the purpose of characterizing the time-varying frequency content of a signal, and they are divided into two classes: the Linear Time-Frequency Transforms and the Quadratic (Bilinear) Transforms.

The bilinear distributions are characterized by a specific kernel function. Due to the bilinearity of these distributions, the signals are expressed as a summation of many components, which usually, when referring to radar signals, overlap in time or frequency; but, unlike the case of linear transforms, this introduces undesirable interfering cross terms, which are troublesome when one wishes to use time-frequency features for pattern recognition. The magnitude and the geometrical characteristics of these cross terms are characterized by the particular kernel function, used in the particular bilinear TF distribution.

This study compares the effects of different kernel functions, as they are employed in various bilinear TF transforms, on Inverse Synthetic Aperture Radar (ISAR) target imaging, in a quantitative way, using a simulated air target radar signal, under several noise conditions.

Radar Imaging of Moving Targets Using Bilinear T-F Signal Transforms

ISAR image formation is the process of reconstructing images of radar targets from recorded radar-received complex data [3–8]. A radar image can be defined as a mapping of a 3D target (e.g. an aircraft) onto a 2D range and cross-range plane. A 2D range and cross-range

image is generated from the recorded data, which are rearranged into a 2D format array that can be easily manipulated computationally (in simulation code).

The end goal is to generate clear ISAR images of moving targets. In order to achieve this, a time-frequency transform with superior resolution and low cross-term interference needs to be devised. Fig. 1 illustrates the process of ISAR image formation (using a wide-band waveform emitted from the radar) based on the time-frequency transform [3]. Having achieved a high-resolution time-varying Doppler spectrum, traditional techniques for obtaining a clear ISAR image (such as ‘range alignment’ and ‘Doppler tracking’ motion compensation techniques) are avoided [3].

Let us assume that the radar transmits a sequence of N pulses. The range resolution is determined by the bandwidth of the emitted pulse. For each transmitted pulse, the total number of range cells, M , is determined by the maximum range covered and the range resolution. The total number of pulses, N , for a given integration time determines the Doppler or cross-range resolution [3]. The time-varying Doppler spectrum can be used to generate a number of range and instantaneous Doppler images.

The cube $Q(r_m, f_n, t_n)$, shown in Fig. 1, is a stack of N image frames and each image frame represents a full range-Doppler image at a particular time.

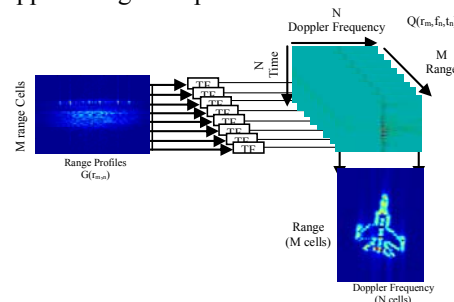


Fig. 1. Time-frequency based image formation

As a final note, it has been recently shown that the so-called 2nd-order Nested Wigner Distribution (NWD) [9] and its marginals have some interesting similarities with the above T-F approach to radar image formation and can offer an alternative method to process radar images for feature extraction and compensations.

Entropy Cost Function

The performance of the various T-F transforms is compared, in a quantitative manner, using the entropy as a cost function, as it seems rather difficult to decide which one is the most efficient for specific radar signals. Our proposed method is to measure the degree of image readability, which mainly refers to clarity or “focus” of the image (signal concentration) and overall resolution, with a specific image cost function based on entropy. The power-normalized image [4, 10] is defined as

$$\bar{\mathbf{I}}_{p,k}(\Phi) = \frac{|\mathbf{I}_{p,k}(\Phi)|^2}{\sum_{p=0}^{N-1} \sum_{k=0}^{K-1} |\mathbf{I}_{p,k}(\Phi)|^2}. \quad (1)$$

Furthermore, the 2-D entropy cost function of the radar image can be defined as

$$H(\Phi) = - \sum_{p=0}^{N-1} \sum_{k=0}^{K-1} \bar{\mathbf{I}}_{p,k}(\Phi) \ln[\bar{\mathbf{I}}_{p,k}(\Phi)]. \quad (2)$$

This cost function is calculated for our example synthetic radar target, for each of the bilinear distributions under consideration and for different SNR values, in order to assess their comparative performance in ISAR imaging. The value of this cost function is always positive, and the smaller it is, the better the quality of imaging obtained.

Bilinear Time-Frequency Transforms

To provide a “baseline level” of performance of a conventional signal analysis method, the 2D Fourier transform was applied, as well as one of the most well known linear time-frequency transforms; the Short Time Fourier Transform (STFT).

The original and most well known bilinear time-frequency transform is the Wigner-Ville Distribution (WVD) [1,2,11]. In the WVD, the time-dependent autocorrelation function is given by

$$\text{WVD}(t, \omega) = \int s\left(t + \frac{t'}{2}\right) s^*\left(t - \frac{t'}{2}\right) \exp\{-j\omega t' t\} dt'. \quad (3)$$

Its application scope is limited mainly due to the so-called ‘cross-term interference’ problem.

In order to reduce the problem of cross-term interference, a large variety of bilinear time-frequency transforms have been proposed in the literature. Of particular importance is the Cohen’s class of bilinear TF transforms [12]. All quadratic TF representations that satisfy the time and frequency shift invariance belong to a general class of distributions introduced by Cohen [14], described by the following generic expression:

$$C(t, f) = \iiint s\left(u + \frac{\tau}{2}\right) s^*\left(u - \frac{\tau}{2}\right) \phi(\theta, \tau) e^{-j2\pi(\theta t + \tau f - \theta u)} d\tau d\theta, \quad (4)$$

where t and f – the time and frequency variables respectively; s – the signal to be processed; s^* – its complex conjugate; τ , u and θ – time and frequency lags; $\phi(\theta, \tau)$ – a two dimensional kernel function, which uniquely characterises the TF distribution $C(t, f)$. This is a generic family of time-frequency distributions, each employing a different two-dimensional kernel function called the ‘parameterization function’. In this study, a number of the well known members of Cohen’s class have been applied and assessed with our radar simulation example.

A prominent member of Cohen’s class is the Pseudo Wigner-Ville Distribution (PWVD). Its mathematical definition is

$$\text{PWVD}(t, \omega) = \int h(t') s(t + t'/2) s^*(t - t'/2) e^{-j\omega t'} dt', \quad (5)$$

where the effect of the time-window $h(t')$ – explained in the literature [14]. The new parameter $h(t')$ – a regular window, which typically causes a frequency smoothing of the WVD.

If we add a degree of freedom in the PWVD by considering a separable smoothing function [7], we allow an independent control, in both time and frequency, of the smoothing that is applied on the WVD. This leads to the following distribution

$$\text{SPWVD}_s^{(g,H)}(t, \omega) = \iint_{t', \omega'} g(t-t') H(\omega - \omega') W_s(t', \omega') dt' d\omega', \quad (6)$$

which is known as the Smoothed Pseudo Wigner-Ville distribution (SPWVD) [12]. The SPWVD allows the smoothing spreads, Δt and $\Delta \omega$, to be adjusted freely and independently of each other. This distribution is defined by a separable smoothing kernel with two windows whose effective lengths independently determine the time and the frequency smoothing spread, respectively [12].

Another commonly applied type of bilinear TF transform - which is also a member of Cohen’s class - is the Choi-Williams Distribution (CWD) [13, 14]. Its exponential kernel is acting like a low pass filter which is expected to reduce the interference terms.

Another member of the Cohen’s class of distributions is the Born Jordan Distribution (BJD). Its mathematical definition is

$$\text{BJ}(t, \omega) = \int \frac{1}{|t'|} \left[\int_{-|t'|/2}^{|t'|/2} s\left(u + \frac{t'}{2}\right) s^*\left(u - \frac{t'}{2}\right) du \right] e^{-j\omega t'} dt'. \quad (7)$$

By smoothing the Born-Jordan distribution along the frequency axis, one can obtain the Zhao-Atlas-Marks distribution [15].

Four other time-frequency distributions (Butterworth, Zhao Atlas Marks, RID and Bessel distributions) were also considered and assessed in terms of their performance in this work. A comparative list of the values of the entropy cost function for all the Time-Frequency methods investigated is given in Table 1.

Looking into the future, apart from these well known bilinear T-F distributions, there has recently been an

increased interest in optimized distributions specially devised to reduce interference. It is only recently that practically applicable schemes have been proposed, offering many opportunities for further research in ISAR imaging. Such schemes can be kernel-independent, e.g. variance-based methods [16], or can involve optimized and signal-dependent kernel design [17,18].

Specification of Radar and Target Parameters

According to [19], a radar target can be considered as a collection of finite number of scattering centers, and its scattered signal can be represented as a superposition of the scattered signals from all scattering centers. Following this model, radar signals from an example synthetic aircraft target are simulated in this work and aircraft ISAR images are calculated using the time-frequency-based image formation method. The simulation code is implemented in the MATLAB environment.

In this paper, the example air target is a simplified model of MIG-25 aircraft, from which raw radar backscattering data are provided and presented in detail in [3]. In particular, the radar is placed on ground and an air target, in general with unknown motion, is to be imaged. The radar operates in the X band with central frequency of 9 GHz. The transmitted radar waveform is a stepped-frequency one, with $M=64$ frequency steps of 8 MHz each, amounting to a total bandwidth of 512 MHz, which corresponds to range resolution equal to $\Delta R = c/2B = 0.29\text{m}$. In our simulated example, we also use $N=512$ bursts (where each burst consists of 64 frequency steps, as described above). The pulse repetition frequency (PRF) is 20,000 pulses/sec. From this data, and using the ISAR imaging method described above, the radar image will consist of 64 range-cells and 512 Doppler frequencies (cross-range cells). For each time-frequency transform considered in this paper, retrieved images for 512 frames will be calculated. As an example, Frame 256 was chosen to be depicted in the figures presented below.

The aircraft (MIG-25) is simulated in two dimensions [3]. It is characterized by 120 point-scatterers, which are distributed in such a way that the periphery of the aircraft is formed. The scatterers are assumed of equal reflectivity.

Finally, the target is assumed to be at a range of 3,500 meters, and its rotation rate to be equal to 10 degrees/sec [3]. Here the rotation is assumed about an axis perpendicular to the ISAR plane, which is defined by the radar line of sight (i.e. the line connecting the radar with the target) and the target's linear velocity vector. The above rotation rate provides a cross-range resolution equal to $\Delta R_{cr} = \lambda/2\psi = 5.79\text{cm}$.

Numerical Results and Comments

In this section we provide numerical results for the radar target described, for different values of signal-to-noise ratio (SNR=40dB, 10dB, 0dB), where the noise is assumed to be Gaussian and white. The image intensity in all figures below is given in linear scale.

In Fig. 2 the ISAR image of the radar target under investigation is shown through the use of a Fourier Transform (FT) based imaging technique [3]. As expected,

the image quality is found here to be rather poor, in comparison with the TF transform-based images provided below, even in the case where no noise is considered.

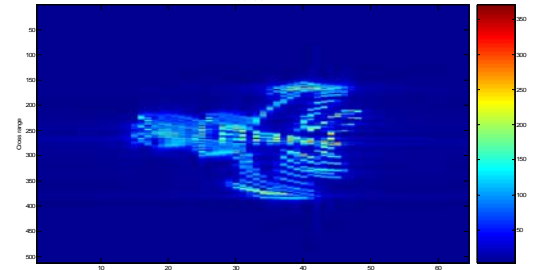
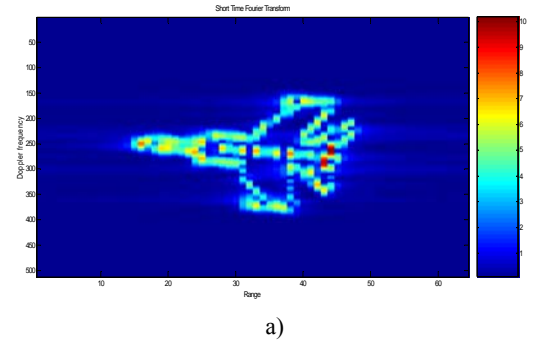
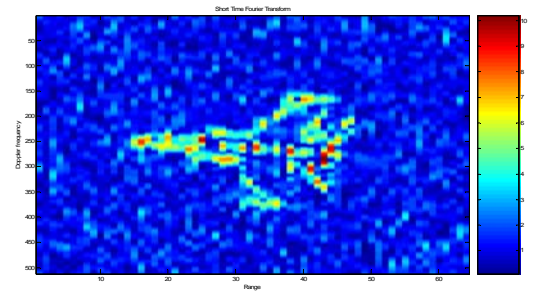


Fig. 2. 2-D Fourier Transform based ISAR image formation



a)



b)

Fig. 3. Short time Fourier Transform (STFT) based ISAR image formation for (a) SNR=40 dB and (b) SNR=0 dB

Furthermore, in Fig. 3 we provide ISAR images of the same target based on the STFT for different values of SNR. Here we can observe, as expected from well known properties of the STFT, a limitation of having good resolution both along the range axis (time), and the cross-range axis (frequency). Indeed, in this particular case (Fig. 3), we can observe a poor localization of the target's point scatterers along the vertical (cross-range/frequency) axis, in contrary to the good scatterers' localization along the horizontal (range/time) axis. In our simulation a 51-point Hamming window is used for time smoothing.

At this point we emphasize that for all time-frequency (TF) distributions that we implement in this paper, the *same* window widths (not necessarily the optimal ones), either in time or in frequency, are used for the purpose of a fair comparison of performance.

Moreover, in Fig. 4 we present numerical results for the same radar target in the case of the Wigner-Ville (WV) bilinear TF transform. Here, we can observe also rather poor reconstructed image quality, in particular in the region around the airplane tail (where most of the target point scatterers have been placed). In addition, the

scatterers are not well localized in the range/cross-range plane, and the interference terms (cross terms) are present at positions where signal energy should be zero.

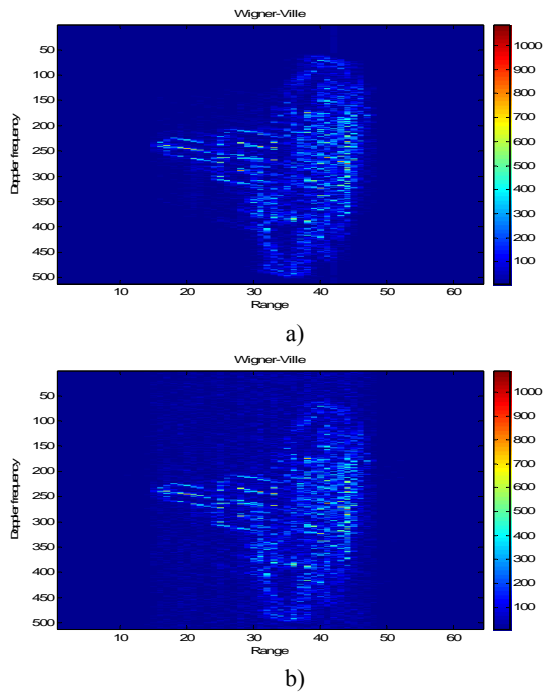


Fig. 4. Wigner-Ville (WV) distribution based ISAR image formation for (a) SNR=40 dB and (b) SNR= 10dB

In Fig. 5, the Pseudo Wigner-Ville (PWV) distribution is presented for SNR values of 40 and 10 dB. As expected, in comparison to the WV-based ISAR image, the image obtained here is more focused and the periphery of the target is obtained rather satisfactorily, at least for the nose and the front side of the wings.

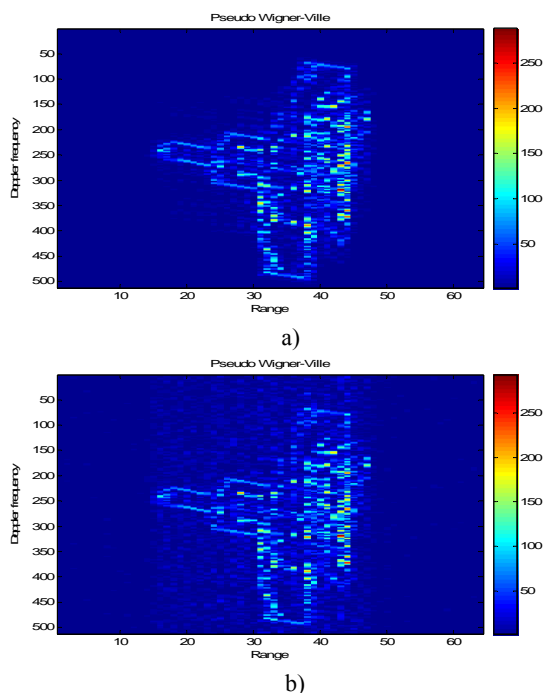


Fig. 5. Pseudo Wigner-Ville (PWV) distribution based ISAR image formation for (a) SNR=40 dB and (b) SNR= 10 dB

Nevertheless, the interference terms still exist and cause intense smearing and poor reconstruction of the back side of the airplane target. For our simulation, a 170-point Hamming window along the time axis is used for the frequency smoothing.

In Fig. 6 we present numerical results for the radar target under consideration in the case of the Smoothed Pseudo Wigner-Ville (SPWV) bilinear TF transform. As expected, due to both time and frequency smoothing, the results are excellent. The target's scatterers are well focused and localized in both time and frequency, and this holds for all three cases of different SNR values. Even in the case of SNR=0 dB we realize that the image reconstruction is still rather satisfactory. For our simulation a 170-point Hamming window along the time axis is used for the frequency smoothing, while a 51-point Hamming window is used for time smoothing.

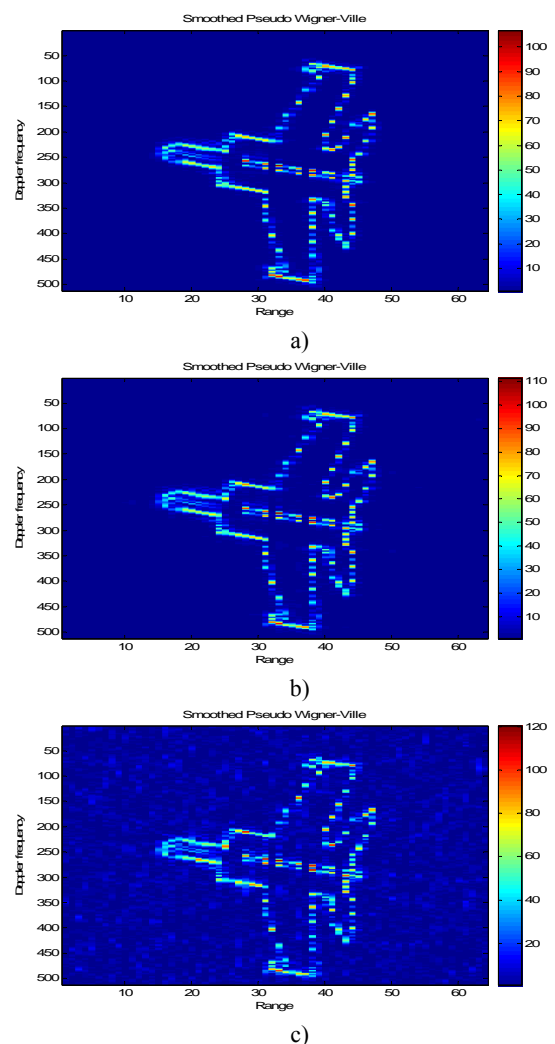


Fig. 6. Smoothed Pseudo Wigner-Ville (SPWV) distribution based ISAR image formation for (a) SNR=40 dB, (b) SNR=10 dB and (c) SNR=0 dB

Moreover, Fig. 7 presents the ISAR imaging result of the radar target for the case of the Choi Williams (CW) distribution. This distribution gives rather adequate results, and we can observe a satisfying localization of the target's point scatterers along both axes, with rather weak blurring appearing for particular range bins along the frequency

(Doppler) axis. In this simulation, a 170-point Hamming window along the time axis was used for the frequency smoothing, and a 51-point Hamming window for time smoothing, whereas the parameter σ (which refers to the kernel's width) is equal to 1 ($\sigma=1$).

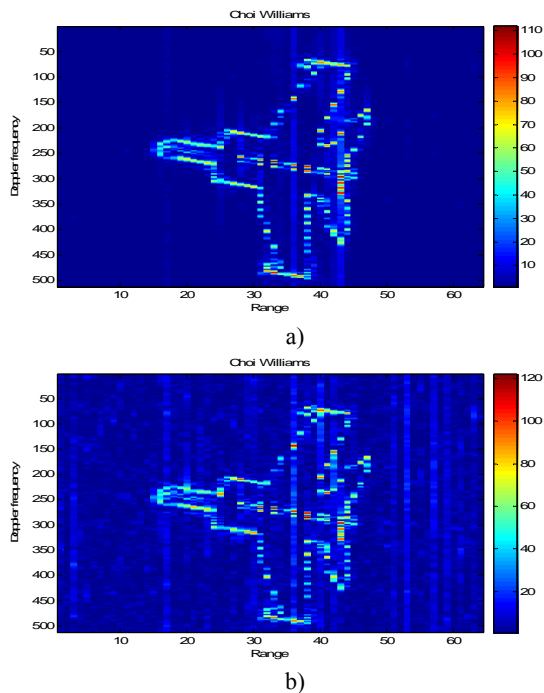


Fig. 7. Choi Williams (CW) distribution based ISAR image formation for (a) SNR=10 dB and (b) SNR=0 dB

Finally, the Born-Jordan, the Butterworth and the Zhao-Atlas-Marks distributions were also simulated in our Matlab environment for ISAR image formation, and they resulted in rather adequate results of accuracy comparable with the Choi-Williams distribution (not shown here).

A comparative list of the values of the entropy cost function for all the TF methods investigated in this paper is given in Table 1. Furthermore, Table 2 shows the computation time for each TF distribution, for a PC Intel Centrino 1.6 GHz, 512 MB RAM. The computation times refer to the imaging procedure, where $M=64$ by $N=512$ input radar data were used for each simulation.

Table 1. Entropy cost function results, indicating ISAR imaging performance

	0 dB	10 dB	20 dB	40 dB
Wigner -Ville	8.9665	7.8941	7.6822	7.6540
Pseudo Wigner - Ville	9.0204	7.8593	7.6054	7.5659
Smoothed Pseudo Wigner - Ville	7.6751	7.0670	7.0322	7.0280
Born Jordan	8.2313	7.3924	7.3219	7.3151
Choi Williams	8.1135	7.3288	7.2935	7.2951
Butterworth	8.1416	7.3442	7.3039	7.3045
STFT	9.4918	8.3482	7.9234	7.8502
RID	8.4711	7.5936	7.4944	7.4780
Bessel	8.4241	7.5635	7.4666	7.4501
Zhao Atlas Marks	7.7956	7.3109	7.2847	7.2809

Table 2. Computation time for TF-based ISAR imaging

Distribution	Computation time (in sec)
Wigner -Ville	9
Pseudo Wigner - Ville	9

Distribution	Computation time (in sec)
Smoothed Pseudo Wigner - Ville	142
Born Jordan	142
Choi Williams	142
Butterworth	142
Short Time Fourier Transform	9
RID	142
Bessel	142
Zhao Atlas Marks	142

Conclusions and Future Research Directions

The most prominent bilinear transform is the Wigner-Ville Distribution, which although it is theoretically optimal, in practice its applicability is limited. Recently a number of other distributions were found to reduce significantly the effects of interference, even though this positive outcome was sometimes mitigated by a relative decrease in the time and frequency resolutions. From the total of ten distributions that were examined using entropy-based comparisons, the Smoothed Pseudo Wigner-Ville was found to give excellent accuracy as far as quality of image reconstruction is concerned, whereas the Choi-Williams, the Butterworth, the Zhao-Atlas-Marks and the Born-Jordan distributions also yielded images of rather high quality and would be recommended for TF-based ISAR imaging. This conclusion is consistent for a range of noise levels, as it was shown in detail.

Regarding future research, more emphasis can be given to the geometry of the target, by using either 3-D CAD models for the aircraft target, or more detailed scattering center representations of them, in which case the Geometrical Theory of Diffraction (GTD) can be used [20,21]. Furthermore, a more complicated target motion will also be examined by our research group in the near future. Finally, another avenue to explore could be to investigate the application of newly proposed, optimized Reduced Interference Distributions (RID, see e.g. [16, 22]), which are applicable to a wide range of radar signal types.

Acknowledgement

The authors would like to thank I. Montiel and C. Garcia of the Research Institute INTA, Spain, for their oral presentation and useful discussions related to this work at an RTA Meeting.

References

1. **Qian S., Chen D.** Joint Time-Frequency Analysis // IEEE Signal Processing Magazine. – 1999. – Vol. 16. – No. 2. – P. 52–67.
2. **Qian S., Chen D.** Joint Time-Frequency Analysis, Prentice Hall. – 1996.
3. **Chen V., Ling H.** Time-Frequency Transforms for Radar Imaging and Signal Analysis, Artech House. – 2002.
4. **Lazarov A., Minchev C.** ISAR Signal Modeling and Image Reconstruction with Entropy Minimization Autofocusing // Proc. DASC 2006.– Portland US. – 2006.
5. **Wehner D.** High-Resolution Radar, Artech House, 2nd edition. – 1995.
6. **Barbarossa S., Scaglione A., Giannakis G.** Product High-Order Ambiguity Function for Multicomponent Polynomial-

- Phase Signal Modeling // IEEE Transactions on Signal Processing. – 1998. – Vol. 46, No. 3. – P. 691–708.
7. **Skrapas K., Boultradakis G., Karakasiliotis A. Frangos, P.** Time – frequency analysis of radar signals for ISAR applications // Proceedings of 2nd International Conference ‘Recent Advances in Space Technologies. – 2005. – P.699–703.
 8. **Karakasiliotis A., Lazarov A., Frangos P., Boultradakis G., Kalognomos G.** Two–dimensional ISAR model and image reconstruction with stepped frequency–modulated signal // IET Signal Processing. – 2008. – Vol. 2. – No. 3. – P. 277–290.
 9. **Qazi S.A., Stergioulas L.K.** Nested Wigner Distributions: Properties and Applications // IEEE Transactions on Signal Processing. – 2006. – Vol. 54. – No. 2. – P. 4662–4674.
 10. **Xi L., Guosui L., Ni J.** Autofocusing of ISAR Images Based on Entropy Minimization // IEEE Trans. Aerospace and Elec. Systems. – 1999. – Vol. 35. – No. 4. – P. 1240–1252.
 11. **Qian S., Chen D.** Decomposition of the Wigner–Ville Distribution and Time–Frequency Distribution Series // IEEE Transactions on Signal Processing. – 1994. – Vol. 42. – No. 10. – P. 2836–2842.
 12. **Hlawatsch F., Boudreaux–Bartels G.F.** Linear and Quadratic Time–Frequency Signal Representations // IEEE Signal Processing Magazine. – 1992. – P. 21–67.
 13. **Auger F., Flandrin P., Goncalves P., Lemoine O.** Time–Frequency Toolbox for Use with Matlab (tutorial). – 1997.
 14. **Choi H., Williams W.** Improved Time–Frequency Representation of Multicomponent Signals using Exponential Kernels // IEEE Trans. Acoust., Speech and Signal Processing. – 1989. – Vol. 37. – No. 6. – P. 862–871.
 15. **Zhao Y., Atlas L. E., Marks, R. J.** The Use of Cone–Shaped Kernels for Generalized Time–Frequency Representations of Nonstationary Signals // IEEE Trans. Acoust., Speech and Signal Processing. – 1990. – Vol. 38. – No. 7. – P. 1084–1091.
 16. **Qazi S.A., Georgakis A., Stergioulas L.K., Shikh–Bahaei M.** Interference Suppression in the Wigner Distribution using Fractional Fourier Transformation and Signal Synthesis // IEEE Transactions on Signal Processing. – 2007. – Vol. 55, No. 6. – P. 3148–3149.
 17. **Baraniuk R.G., Jones D.L.** A Signal Dependent Time–frequency Representation: Optimal Kernel Design // IEEE Transactions on Signal Processing. – 1993. – Vol. 41. – P. 1589–1601.
 18. **Ristic B. Boashash B.** Kernel Design for Time–frequency Signal Analysis Using the Radontransform // IEEE Transactions on Signal Processing. – 1993. – Vol. 41. – P. 1996–2008.
 19. **Odendaal J., Barnard E., Pistorius C.W.** Two–Dimensional Superresolution Radar Imaging Using the MUSIC Algorithm // IEEE Trans. Ant. and Propagation. – 1994. – Vol. 42. – No. 10. – P. 1386–1391.
 20. **Potter L. C., Chiang D. M., Carriere R., Gerry, M. J. A** GTD–Based Parametric Model for Radar Scattering // IEEE Transactions on Antennas and Propagation. – 1995. – Vol. 43. – No. 10. – P. 1058–1067.
 21. **Gerry M. J., Potter L. C., Gupta I. J., Merwe A.** “A Parametric Model for Synthetic Aperture Radar Measurements // IEEE Transactions on Antennas and Propagation. – 1999. – Vol. 47. – No. 7. – P. 1179–1188.
 22. **Stankovic L. J.** The auto–term representation by the reduced interference distributions: The procedure for a kernel design // IEEE Transactions on Signal Processing. – 1996. – Vol. 44. – No. 6. – P. 1557–1564.

Received 2009 02 12

G. E. Boultradakis, G. K. Kalognomos, A. V. Karakasiliotis, P. V. Frangos, L. K. Stergioulas. A Comparative Study of Bilinear Time–Frequency Transforms of ISAR Signals for Air Target Imaging // *Electronics and Electrical Engineering*. – Kaunas: Technologija, 2009. – No. 4(92). – P. 87–92.

In this paper a comparative study of bilinear time–frequency (TF) transforms for Inverse Synthetic Aperture Radar (ISAR) imaging is presented. Following a concise presentation of the ISAR imaging method used in this work, as well as of the theory of the bilinear TF transforms involved in our numerical simulations, extended numerical results are presented for a reference simulated radar target and for various noise conditions. The constructed ISAR images are presented and analyzed quantitatively using an entropy cost function criterion, while corresponding run–time considerations have also been taken into account. As a result, it appears that the Smoothed Pseudo Wigner–Ville (SPWV) distribution provides us with images of superior quality. Furthermore, the analysis of the results demonstrates the usefulness of bilinear TF methods in ISAR imaging and showcases the relative performance advantages and disadvantages of the various distributions. Ill. 7, bibl. 22 (in English; summaries in English, Russian and Lithuanian).

Г. Е. Болтадакис, Г. К. Калогномос, А. В. Каракасилотис, П. В. Франгос, Л. К. Стергиолас. Сравнительное исследование сигналов билинейного время–частотного преобразования в возвратном радаре синтезированной апертуры при решении задач обработки изображений // *Электроника и электротехника*. – Каунас: Технология, 2009. – № 4(92). – С. 87–92.

В статье приведено сравнительное исследование сигналов билинейного время–частотного преобразования в возвратном радаре обратной синтезированной апертуры при обработке изображений. После краткой презентации метода синтезированной апертуры изображений, используемого в этой работе, а также теории билинейных время–частотных преобразований показаны возможности при численном моделировании. Результаты численного моделирования представлены для имитируемых радиолокационных целей при различных уровнях шума. Построенные обратной синтезированной апертуры изображения оценены и проанализированы при помощи функции количественной энтропии, критерия стоимости, принимая во внимание продолжительность выполнения. В результате выясняется, что распределение дает изображения высшего качества. Кроме того, анализ результатов свидетельствует о целесообразности применения билинейных время–частотных преобразований в обратной синтезированной апертурой изображений и относительно высокой эффективности, по сравнению с другими методами. Ил. 7, библи. 22 (на английском языке; рефераты на английском, русском и литовском яз.).

G. E. Boultradakis, G. K. Kalognomos, A. V. Karakasiliotis, P. V. Frangos, L. K. Stergioulas. Dvitiesės laiko ir dažnio transformacijos lyginamasis signalų tyrimas sintezuotosios apertūros grįžtamajame radare // *Elektronika ir elektrotechnika*. – Kaunas: Technologija, 2009. – Nr. 4(92). – P. 87–92.

Šiame darbe atliktas dvitiesės laiko ir dažnio transformacijos sintezuotosios apertūros grįžtamajame radare lyginamasis signalų tyrimas taikant tikslinį oro vaizdų apdorojimą. Trumpai apibūdinti šiame darbe taikomi ISAR vaizdų metodai, taip pat dvitiesės teorijos dažnio transformacijos. Pateikiami įvairūs modeliavimo rezultatai, tarp jų ir gauti įvairiomis triukšmo sąlygomis. Pateikti ISAR vaizdai analizuojami kiekybiniu požūriu taikant entropijos funkciją, taip pat ir atsižvelgiant į laiko faktorių. Iš pateiktų rezultatų matyti, kad Wigner–Ville pseudopasiskirstymas duoda aukščiausios kokybės vaizdus. Iš gautų rezultatų matyti dvitiesio laiko ir dažnio metodo naudingumas, palyginti su kitais pasiskirstymo metodais. Il. 7, bibl. 22 (anglų kalba; santraukos anglų, rusų ir lietuvių k.).